Modelling of Hot Rotary Kiln

Dmitrij Ramanenka[1], Gustaf Gustafsson[1], Pär Jonsén[1]

[1]Luleå University of Technology

Abstract

Rotary kilns are the central part in the production of many important materials, such as: cement clinkers, lime for paper production and iron-ore pellets for steel making. The main design of a rotary kiln is rather simple – consisting of a cylindrical steel casing and one or several layers of refractories in order to protect the casing from high service temperatures. The dimensions of a rotary kiln vary between some 10 to 180 m in length and 2 to 8 m in diameter. Damage to the refractory lining is common and can potentially lead to long-lasting production shut-downs and high production losses. Due to the harsh inner environment and the large dimensions of the kiln it is difficult to observe and evaluate the kiln while in service – hindering improvement of the kiln. Therefore, it is advantageous to perform computer simulations and potentially improve the design of refractories (bricks), the material choice and operation of the kiln based on the numerical results.
In this work, LS-DYNA is used for simulation of a hot rotary kiln insulated with a single lining of refractory bricks. A cross-section of a kiln of approximately 8 m in diameter is modelled. The physical time to model is up to 65 h. The model is time-dependent and includes thermal expansion and rotation of the kiln. Heat transfer coefficients are calibrated by LS-OPT. It is found that modelling of a hot rotary kiln is rather successful, but several challenges exist. Calculation time can in some cases reach 2-3 weeks (implicit, MPP, 16 cores). Instabilities due to contact associated problems are common. The created model facilitates decision making regarding e.g. heating/cooling procedure, design changes, maintenance frequency and more.

1 Introduction

Manufacturing of many different products involves elevated temperatures. Rotary kilns are designed to maintain high temperatures and to handle relatively large volumes of material in a continuous manner. Some of the well-known products are: cement clinkers, iron-ore pellets and lime.

A rotary kiln typically consists of a cylindrical steel casing and one or several layers of refractories in order to protect the casing from high service temperatures which are typically above 1000 °C. The casing is bounded by a pair of riding tyres which are resting on the riding wheels and so called pads separate casing from the riding tyres acting as sacrificing abrasion material. The dimensions of a rotary kiln ranges approximately between 10 to 180 m in length and 2 to 8 m in diameter, see Fig.1: for illustration.

The conditions inside a kiln are rough and damage to the refractory lining is inevitable in the long-run. Regular maintenance is planned in advance typically around 12 month apart. However, unpredicted failures of the lining happening before the planned maintenances are common. This can be very troublesome to a company, repair time is long (5-14 days) and can become very costly.

Due to the high temperatures and the large dimensions of a rotary kiln it is difficult to study a kiln in-situ. In this work, creation of a FE-model of a large, hot rotary kiln using LS-Dyna is suggested. With a numerical model some inconveniences of the size of a kiln and high temperatures can be overcome and potential improvements of the kiln can be tested.

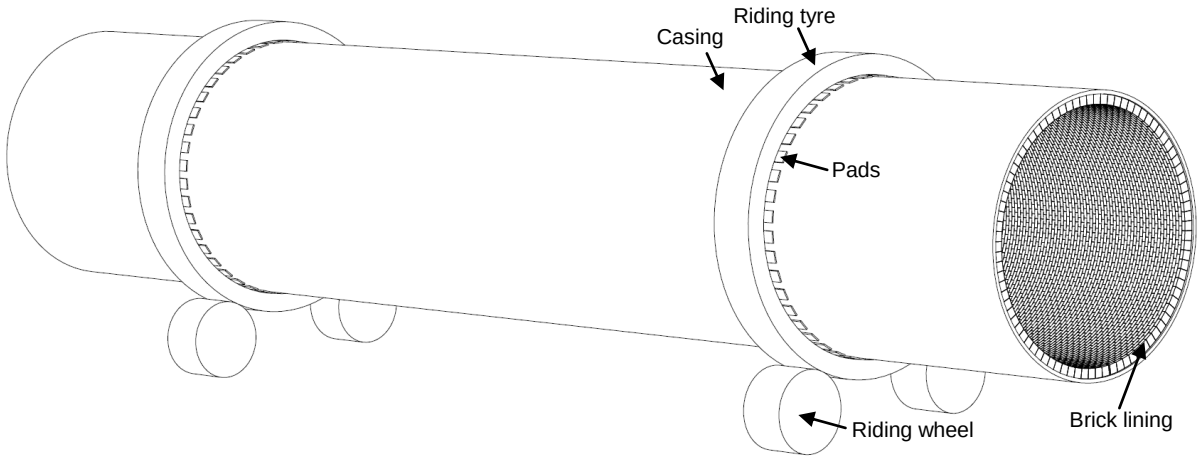

Fig.1: Illustration of a rotary kiln lined with a single brick layer.

2 Method of model creation

The aim of the model is to be able to simulate a hot rotary kiln with time-dependent heat transferring. The problem to solve is a coupled non-linear structural thermal analysis.

2.1 Dimensions

The model studied is a cross-section of the kiln with a single layer of brick lining having thickness of 100 mm. It is thus a 3-dimensional model. The geometry is presented in Fig.2:.

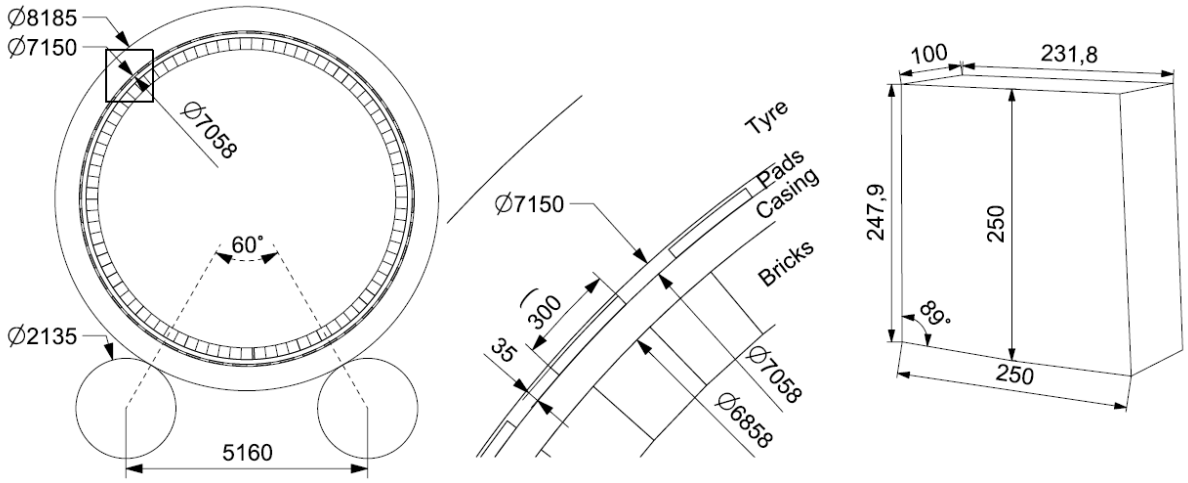

Fig.2: Dimensions of the model.

The choice of the model is based on the fact that statistically most of the failures of the lining happen around the area of the lower pair (closest to the flame) of riding wheels [1]. Additionally, handling of boundary conditions is straight forward because of the riding wheels.

2.2 Element type and mesh

Fully integrated quads (**`*SECTION_SOLID`** *ELFORM=2*) having mesh of 22-26 mm where used in the discretization of the geometry. Mesh representation can be seen in Fig.3:. Total number of elements reaches approximately 126000.

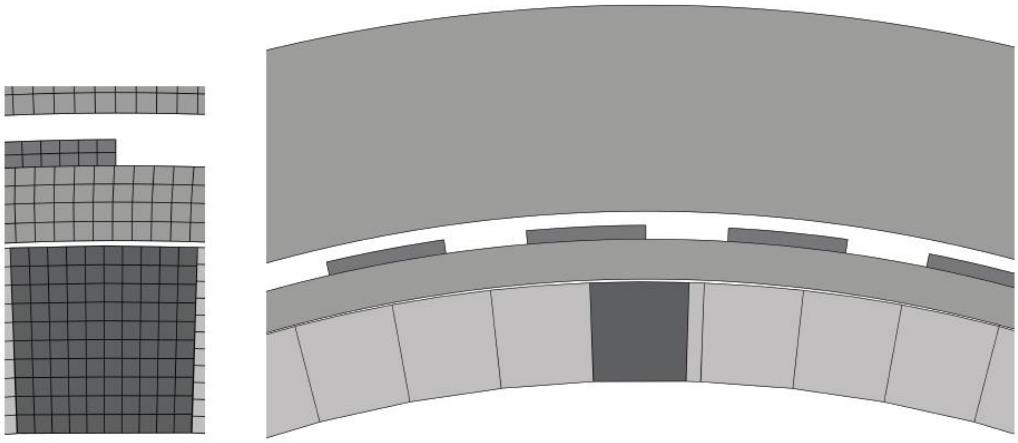

Fig.3: Illustration of the mesh (22-26 mm).

2.3 Integration method

Due to the long simulation times the tasks associated with rotary kilns are usually solved implicitly. In some cases e.g. during stress updates it can be advantageous to start numerical integration explicitly and switch to the implicit integration later on. Fig.4: shows typical settings in order for implicit integration to run properly, controlled by the card: ***CONTROL_IMPLICIT_SOLUTION.**

***CONTROL_IMPLICIT_SOLUTION**

1	NSOLVR	ILIMIT	MAXREF	DCTOL	ECTOL	RCTOL	LSTOL	ABSTOL
	12	11	15	0.0010000	0.010000	1.000e+10	0.9000000	1.000e-20
2	DNORM	DIVERG	ISTIF	NLPRINT	NLNORM	D3ITCTL	CPCHK	
	2	1	1	0	1.0000000	0	0	
3	ARCCTL ●	ARCDIR	ARCLEN	ARCMTH	ARCDMP	ARCPSI	ARCALF	ARCTIM
	0	0	0.0	1	2	0	0	0
4	LSMTD	LSDIR	IRAD	SRAD	AWGT	SRED		
	5	2	0.0	0.0	0.0	0.0		

Fig.4: Typical settings for activation of implicit integration.

2.3.1 Convergence

In case of convergence problems one solution can be to lower the default value of *ECTOL* in ***CONTROL_IMPLICIT_SOLUTION.**, e.g. by factor 10.

Activation of the card ***CONTROL_IMPLICIT_DYNAMICS** helps in many cases to resolve convergence troubles. Additionally, it may be beneficial to induce artificial damping by increasing the default values of Newmark integration parameters, *GAMMA* and *BETA*, see example in Fig.5:.

***CONTROL_IMPLICIT_DYNAMICS**

1	IMASS ●	GAMMA	BETA	TDYBIR	TDYDTH	TDYBUR	IRATE
	1	0.6000000	0.3800000	0.0	1.000e+24	1.000e+24	0

Fig.5: Example of inducing of numerical damping by increasing GAMMA and BETA. Default and minimum of GAMMA and BETA is 0.5 and 0.25, respectively.

2.4 Gravitational preload

The cross section of the casing is oval due to the gravity force, see illustration in Fig.6:. Due to the ovality a gravitational preload needs to be applied before brick lining can be introduced into the casing, see Fig.7:a.

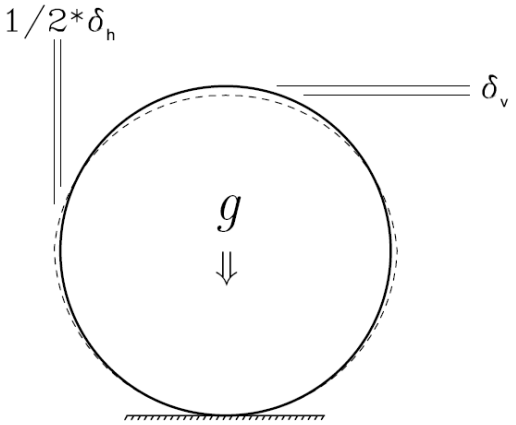

Fig.6: Illustration of the ovality of the casing [2].

2.4.1 Analytical verification

At this stage a verification of the model's response can be performed. For example could a FE-model of the case in Fig.6: be created and deformation of the casing found numerically compared to the analytical solution, see equation 1 and 2, respectively. Convergence test of the mesh could be as well performed. Satisfactory results verified analytically confirm proper model build up before continuation. For more details see [2].

$$\delta_h = 0.429 \frac{12 \cdot \rho g r^4}{E t_C^2} \tag{1}$$

$$\delta_v = 0.467 \frac{12 \cdot \rho g r^4}{E t_C^2} \tag{2}$$

Where δ_h and δ_v are horizontal and vertical displacements, ρ is density, g is standard gravity, r is the nominal inner radius, E and t_C are Young's modulus and thickness of the casing, respectively.

Stresses from the preload are saved and included in the next step – bricklaying.

2.5 Bricklaying

In practice the bricks are positioned in the kiln one by one. It is advantageous to update the stresses few times during the bricklaying while modelling in order to mimic the reality; Fig.7: shows the principle of bricklaying with stress updates. For more details see [2].

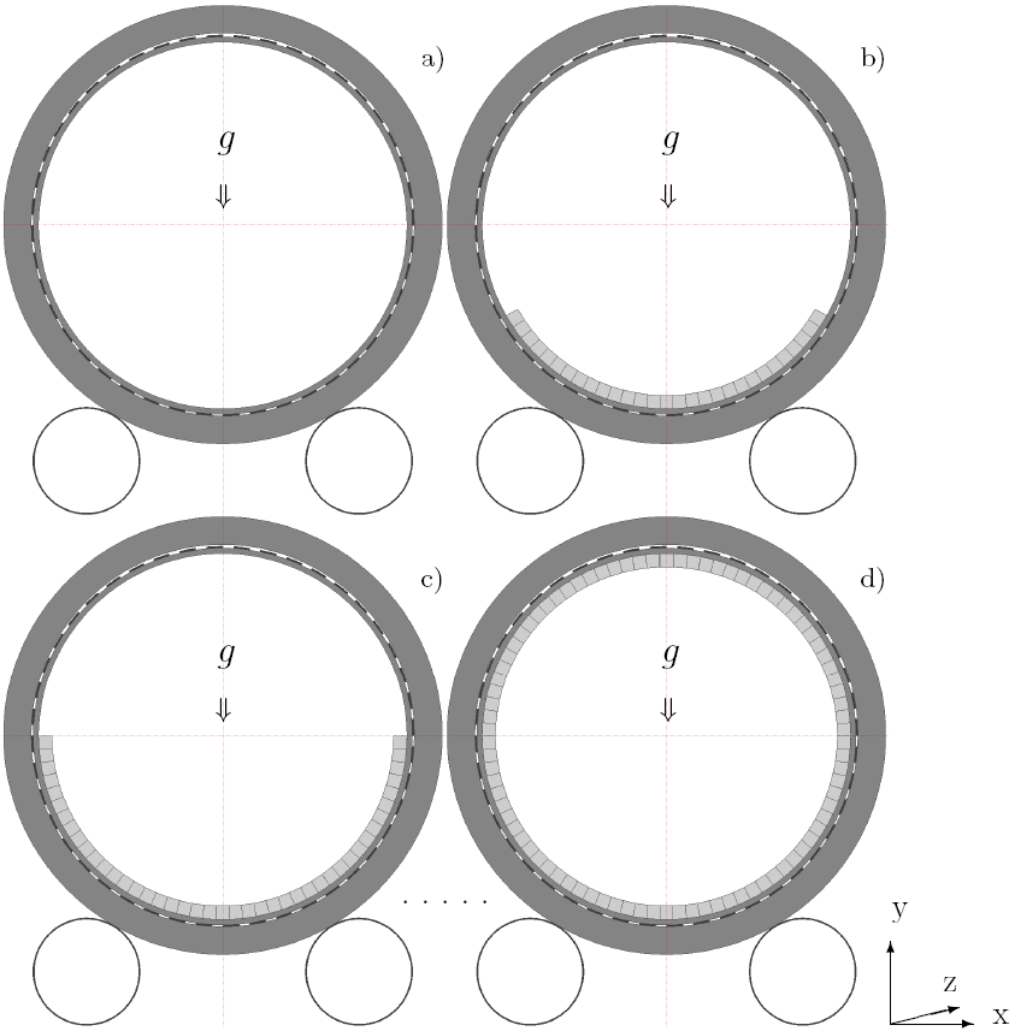

Fig.7: Example of bricklaying sequences with stress update in between [2].

2.6 Contact

For the contact between the bricks the card ***CONTACT_AUTOMATIC_SINGLE_SURFACE_MORTAR** was activated. For the contact between pads and the casing the card ***CONTACT_AUTOMATIC_SURFACE_TO_SURFACE_MORTAR_TIED** was activated. For the remaining contacts the card ***CONTACT_AUTOMATIC_SURFACE_TO_SURFACE_MORTAR** was used.

Mortar contact is a segment to segment penalty based method that was specifically designed to make implicit integration more stable. However, due to its smooth contact properties it may tend to result in larger penetration between the parts compared to the traditional penalty based method used in the explicit integration. When regarding simulation of the kiln this is especially noticed during thermal expansion of the kiln.

Regard a simple penetration test in Fig.8: with default settings in the contact card. The test shows expansion of two elements clamped in one direction that are heated 1300 °C in 10 seconds; linear expansion coefficient is $6 \cdot 10^{-6}$.

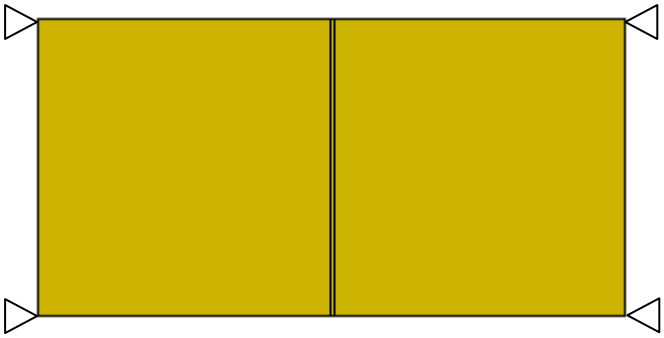

Fig.8: Example of penetration problem during expansion using default settings in the mortar contact card.

The test shows that penetration is severe. In order to battle the problem one can change default settings in the contact card. The parameters to consider are *SFS, SFM, SST* and *MST*. See an example in Fig.9: of how to change parameters in order to solve penetration problem in the presented penetration test. The choice of parameters should satisfy the analytical solution for the induced compressive stress.

***CONTACT_AUTOMATIC_SINGLE_SURFACE_MORTAR**

6	SFS	SFM	SST	MST	SFST	SFMT	FSF	VSF
	10.0000000	1.0000000	1.000e-10	1.000e-10	1.0000000	1.0000000	1.0000000	1.0000000

Fig.9: Example of how penetration problem in the penetration test, Fig.8:, can be battled by changing default values of SFS, SST and MST.

2.7 Rotation of the kiln

Rotation of the kiln is induced by the rotation of the riding wheels, which due to their high-stiffness are considered as rigid. Activation of rotation is handled by the card: ***BOUNDARY_PRESCRIBED_MOTION_RIGID**.

2.8 Heating

2.8.1 Time-independent heating

For a steady state solution the heating of the kiln is solved by applying temperature at the boundary nodes of the present parts, see Fig.10:. This is activated by the card: **BOUNDARY_TEMPERATURE_SET**.

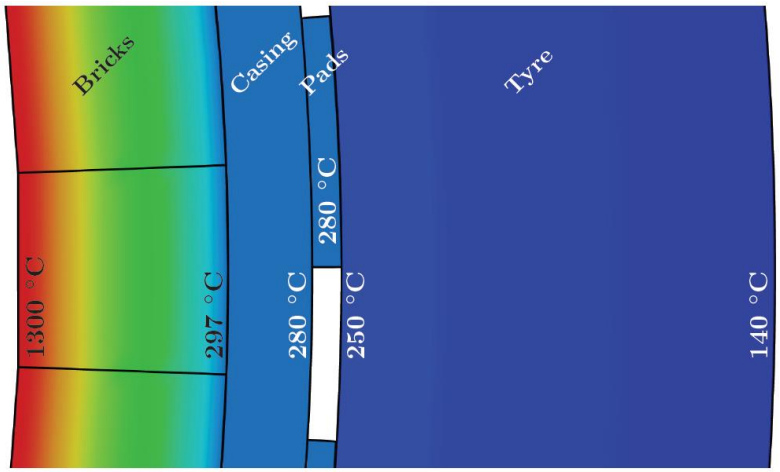

Fig.10: Example of boundary temperature conditions for a steady-state solution [3].

2.8.2 Time-dependent heating

In order to make heating of the kiln time-dependent knowledge of heat transfer coefficients is required. This includes radiation, convection and conduction coefficients. If the development of the temperature on the hot face of the bricks as well as on the cold face of the tyre is known, the heat transfer parameters in the model can be calibrated towards that. Fig.11: illustrates the time-dependent heating of the model.
Radiation and convection heat transfer coefficients between the surfaces can be approximated based on the information from literature. For that the emissivity coefficients of the surfaces and thermal conductivity of the air between the surfaces are required.
Free surface heat loss (radiation and convection) and conduction heat transfer coefficients are more complicated to approximate. For that purpose it is advantageous to use an optimization software, such as LS-OPT, that can iterate the best solution to match the temperature development of the cold face of the tyre. It is true that the heat transfer coefficients found by LS-OPT may not be very close to the true values. However, the main purpose is to obtain similar heating rate of the cold face of the tyre as in reality. It is not of interest to know e.g. whether cooling of the tyre is dominated by radiation or convection heat loss.

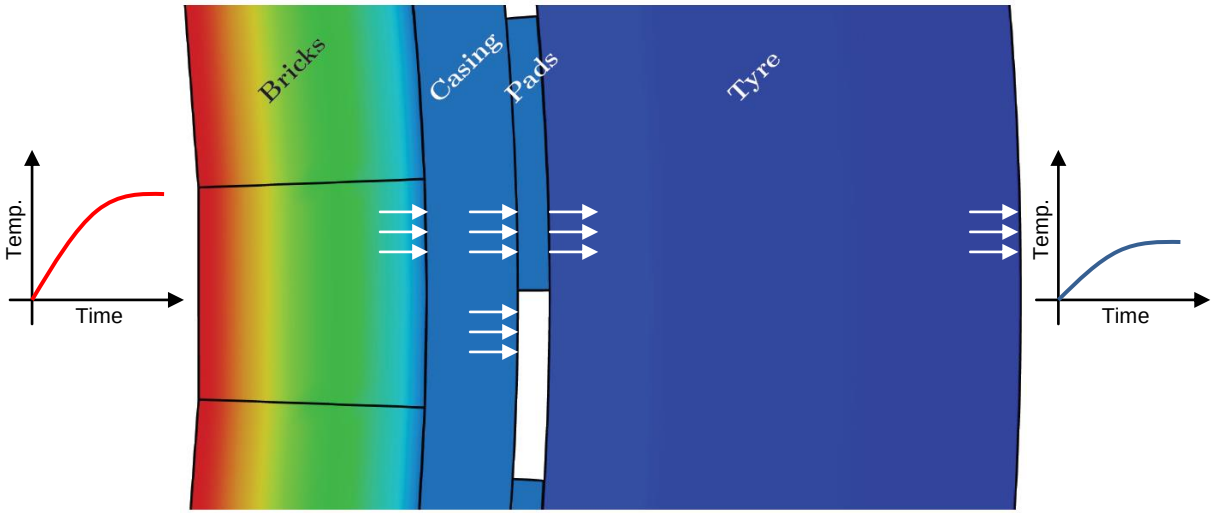

Fig.11: Illustration of the temperature development on the hot face of the bricks and the cold face of the tyre and the heat transfer boundaries.

3 Results

3.1 Overview of thermal stresses in the brick lining

Fig.12: and Fig.13: shows development of highest compressive and tensile stresses in the brick lining during heating of the kiln, respectively. It is seen that highest compressive stress is close to the hot surface of the bricks. Approximately after 20.5 hours of heating, the compressive stress band starts to move deeper. When the steady state is reached the highest compressive stress is some 100 mm below the hot face of the brick. The tensile stress is rising steadily until it reaches maximum at steady state. The results show that it is rather important to be able to simulate time-dependent events. The compressive stresses during heating stage are considerably higher than at steady state – reaching up to half of the bricks compressive strength. Further on, the peaks of compressive stress can be related to a certain time or temperature – helping to reconsider the heating procedure. The question to be asked could be: Should the kiln be rotated (typical procedure during heating) before certain temperature of the tyre is reached? Could it be possible to increase heating rate after a certain temperature of the tyre is reached?

.

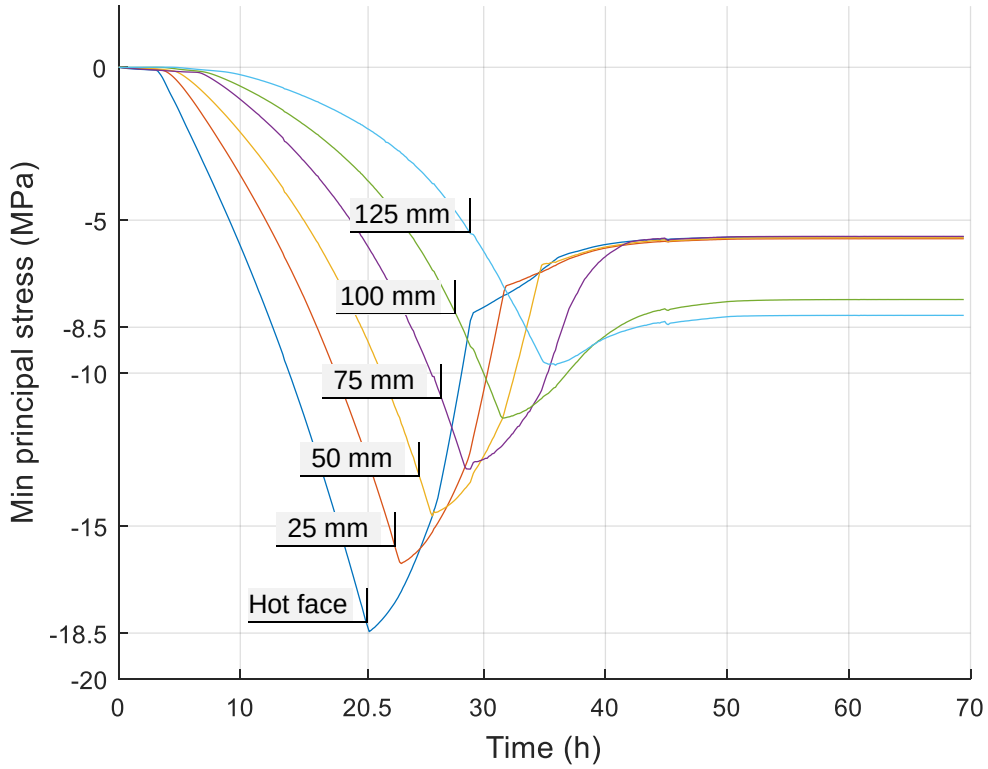

Fig.12: Development of highest compressive stresses in the brick lining during heating of the kiln. The values mark the depth from the hot face of the bricks.

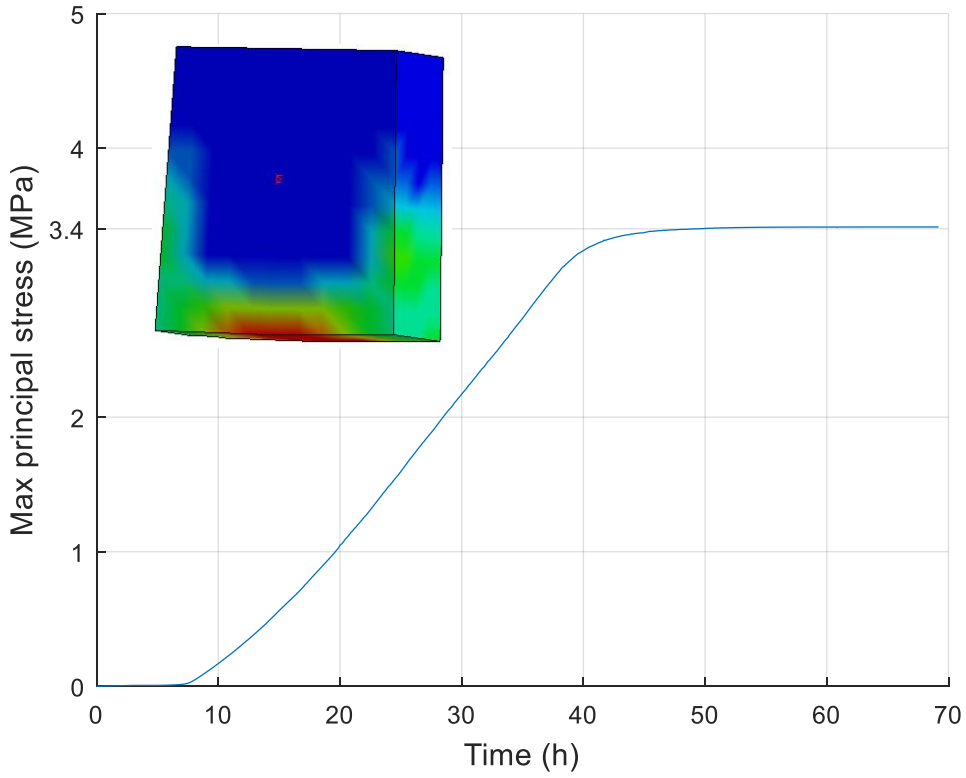

Fig.13: Development of highest tensile stresses in the brick lining during heating of the kiln. Location of the highest tensile stresses is along the contact line of the neighboring bricks and at the bottom of the bricks in contact with the casing, see the included image.

4 Summary

The primary purpose of this work was to propose a way of modelling and simulating hot rotary kiln by using LS-Dyna. It was shown what geometry and what discretization choice is reasonable. The methodology of bricklaying and heating of the kiln is proposed. It is shown some of the important settings in LS-Dyna in order for the model to run properly. It is suggested some ways of overcoming convergence and contact problems.

Results presented in this work show development of highest compressive and tensile stresses in the brick lining during heating of the kiln. The data facilitates decision making e.g. regarding potential improvement of the heating scheme in this particular case. In general, the model has a great potential for supporting engineers with additional information that is difficult to obtain in-situ.

5 Literature

[1] Shubin, V: "Mechanical effects on the lining of rotary cement kilns", Refract. Ind. Ceram, 42, 2001, 245-250

[2] Ramanenka, D., Stjernberg, S., Jonsén P.: "FEM investigation of global mechanisms affecting brick lining stability in a rotary kiln in cold state", Eng. fail. Anal., 59, 2015, 554-569

[2] Ramanenka, D., Antti M-L., Gustafsson G., Jonsén P.: "Characterization of high-alumina refractory bricks and modelling of hot rotary kiln behaviour", submitted to Eng. fail. Anal.